

I.

A.

1.

This figure "fig_1.png" is available in "png" format from:

<http://arxiv.org/ps/2305.04725v2>

Wide Test Figure

Thin channel Ga₂O₃ MOSFET with 55 GHz f_{MAX} and >100 V breakdown

Chinmoy Nath Saha,¹ Abhishek Vaidya,¹ Noor Jahan Nipu,¹ Lingyu Meng,² Dong Su Yu,² Hongping Zhao,² and Uttam Singiseti¹

¹Electrical Engineering, University at Buffalo, Buffalo, New York 14240, USA

²Electrical and Computer Engineering, Ohio State University, Columbus, OH 43210, USA

(*Electronic mail: uttamsin@buffalo.edu)

(Dated: 16 November 2023)

This letter reports a highly scaled 90 nm gate length β -Ga₂O₃ (Ga₂O₃) T-gate MOSFET with power gain cut off frequency (f_{MAX}) of 55 GHz. The 60 nm thin epitaxial Ga₂O₃ channel layer was grown by molecular beam epitaxy (MBE) while the highly doped (n++) source/drain regions were regrown using metal organic chemical vapour deposition (MOCVD). Maximum on current ($I_{\text{DS, MAX}}$) of 160 mA/mm and trans-conductance (g_{m}) around 36 mS/mm was measured at $V_{\text{DS}} = 10$ V for $L_{\text{SD}} = 1.5$ μm device. Transconductance and on current are limited by high channel sheet resistance (R_{sheet}). Gate-drain breakdown voltage of 125 V was measured for $L_{\text{GD}} = 1.2$ μm . We extracted 27 GHz current gain cut-off frequency (f_{T}) and 55 GHz f_{MAX} for 20 V drain bias for unpassivated devices. The reported f_{MAX} is the highest for Ga₂O₃. While no current collapse was seen initially for both drain and gate lag measurements for 500 ns pulse, moderate current collapse was observed after DC, RF measurements caused by electrical stressing. No large signal RF data was extracted due to a lack of proper tuning of the input (high S11) in the load-pull setup. However, after repeated DC and large signal measurement trials, we found that both f_{T} and f_{MAX} degraded significantly which was correlated to high-frequency g_{m} collapse. Despite this, we calculated a high f_{T} . V_{BR} product of 3.375 THz.V which is comparable with state-of-art GaN HEMTs. This figure of merit suggests that Ga₂O₃ could be a potential candidate for X-band application.

β -Ga₂O₃ (Ga₂O₃) is an ultrawide bandgap semiconductor with favorable materials properties¹ for next-generation power and RF applications. The predicted breakdown field (8 MV/cm)^{1,2} and calculated saturation velocity³ supports the candidacy of Ga₂O₃ for high-frequency switching and high power RF amplifier applications. β -Ga₂O₃ MOSFETs with multi-kV breakdown voltages have been reported⁴⁻⁸, while heterostructure FET (HFET), and diodes with average breakdown field strength of 5.5 MV/cm^{9,10} has been reported demonstrating the maturity of the technology. Modulation doped β -(Al_xGa_{1-x})₂O₃/Ga₂O₃ HFET¹¹ and highly scaled (< 200 nm) MOSFETs¹² and MESFETs¹³ have been demonstrated to showcase the high-frequency performance. In our previous works, we reported $f_{\text{T}} = 30$ GHz in Al-GaO/GaO HFETs^{14,15} and $f_{\text{MAX}} = 48$ GHz using scaled T gate MOSFET¹⁰. Large signal RF performance has been published for L-band¹⁶. However, $f_{\text{MAX}} > 50$ GHz is necessary for S and X band applications.

It is necessary to reduce the parasitic source resistance to achieve higher frequencies. The contact regrowth process has been reported in gallium oxide FETs^{10,14,15} as an effective way to reduce contact resistance. In our previous report, we found high regrowth interface resistance¹⁰ limiting device performance by increasing source resistance. Careful surface treatment could reduce this regrowth interface resistance problem. Traps in the gate and gate-drain access region can limit device RF performance by introducing current collapse known as DC-RF dispersion¹⁰. Ex-situ passivation can eliminate the access region traps but traps under the gate are unaffected by passivation¹⁷.

In this letter, we report highly scaled 90 nm T-gate Ga₂O₃

MOSFET with improved MOCVD contact regrowth process to reduce the interface resistance. Pre-cleaning of the wafer before low-temperature n++ regrowth gave lower interface resistance. We used atomic layer deposited Al₂O₃ as the gate dielectric, no current collapse was observed in unpassivated devices. As a result, a peak f_{T} of 27 GHz and $f_{\text{MAX}} = 55$ GHz is obtained in these devices. With a gate-to-drain breakdown voltage of 120 V, the device shows $f_{\text{MAX}} = 55$ GHz and breakdown voltage ($V_{\text{BR}} > 100$ V which has been reported only in a few state-of-art AlGaIn/GaN HFETs¹⁸⁻²⁰.

The device layers and structure is shown in Fig. 1 (a). The growth details and device fabrication process is described in detail in previous reports^{10,21}. Before regrowth, the sample was submerged in 1:3 HCl:DI water solution for 15 minutes to remove any atmospheric contaminants⁶. Next, 80 nm highly Si doped (1×10^{20} cm⁻³) n++ layer was grown using MOCVD at a lower 650 °C. Unlike the previous report¹⁰, a 20 nm aluminum oxide gate dielectric was used in these MOSFETs. SEM image of the device is shown in Fig. 1 (b), a T-gate was used to improve the gate resistance.

From the capacitance-voltage characteristics (Supplementary material), a sheet carrier charge density (2.9×10^{12} cm⁻²) was extracted. Transfer length method (TLM) on n++ regrowth layer gave a 0.045 Ω mm lateral contact resistance ($R_{\text{c,n++}}$) between metal and n++ layer and a sheet resistance ($R_{\text{sheet,n++}}$) of 181 Ω/\square . TLM structure on n++ layer through the channel was also fabricated to calculate total contact (R_{C}) resistance to the channel. We extracted a low metal to channel contact resistance (R_{C}) of 0.624 Ω mm and a channel sheet resistance ($R_{\text{sheet, ch}}$) of 28 K Ω/\square . Lower contact resistance (R_{C}) compared to previous report¹⁰ suggests that the surface

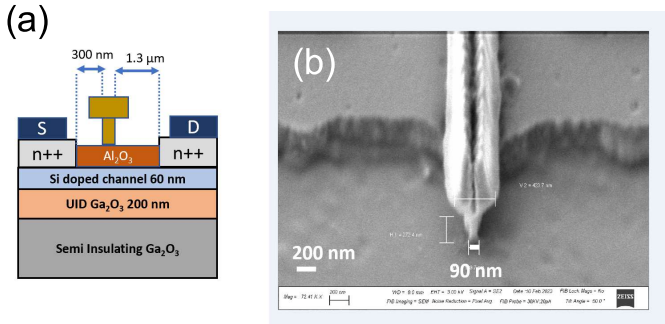


FIG. 1. (a) Cross section schematic of a MOSFET (b) Magnified SEM image of a fabricated device showing 90 nm T gate with 450 nm Gate hat

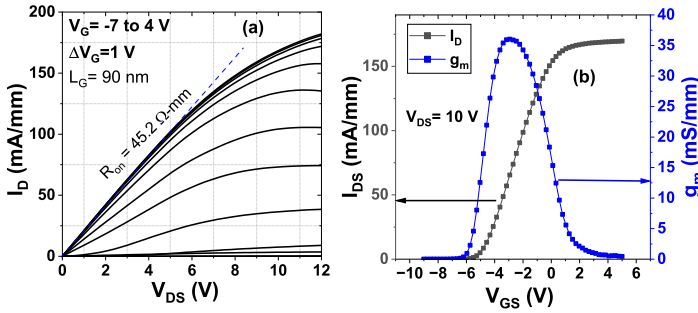


FIG. 2. (a) I_D - V_{DS} output curve for a $L_G= 90$ nm device (b) I_D - V_{GS} transfer curve at $V_{DS}= 10$ V showing 36 mS/mm transconductance

treatment and low temperature regrowth were helpful.^{6,22}

DC I_D - V_{DS} output curves shows peak $I_{DS,MAX} = 182$ mA/mm with $45.2 \Omega \text{ mm}$ at $V_{DS} = 12$ V (Fig. 2 (a)). Peak transconductance (g_m) was found 37 mS/mm at 10 V drain bias (Fig. 2 (b)). However, only 10 V drain bias was used for transfer curve in order to avoid stressing the device. Higher R_{on} and lower g_m for $L_G < 100$ nm can be attributed to higher channel sheet resistance which increases source resistance (R_S) compared to the previous report. Three terminal off-state

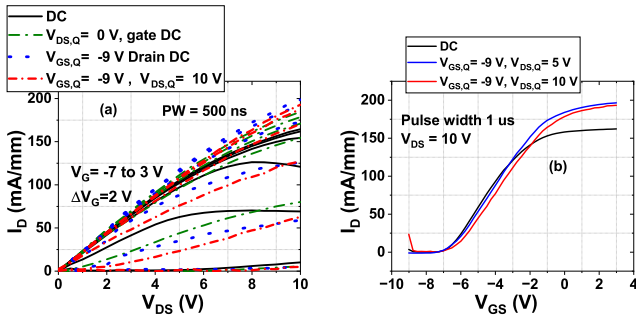


FIG. 3. (a) I_D - V_{DS} output curve for different gate and drain quiescent bias points showing no current collapse (b) I_D - V_{GS} transfer curve of the device showing no current collapse at higher gate-drain quiescent point for $1 \mu\text{s}$ pulse width

breakdown measurement was carried out in air using B1505A power device analyzer. The device was biased at $V_{GS} = -15$ V which is below V_{TH} . We observed catastrophic breakdown at $V_{DS} = 110$ V (supplementary material), which corresponds to gate-to-drain breakdown voltage (V_{BR}) of 125 V ($V_{DS} - V_{GS}$). It results in 1.18 MV/cm average breakdown field (E_{AVG}) for $1.26 \mu\text{m}$ L_{GD} spacing. Lower E_{AVG} can be explained due to air breakdown and lack of external passivation and field management.

Pulsed-IV measurements were carried out using Auriga-AU5 pulse voltage system with low duty cycle to reduce self-heating. No current collapse was observed and pulsed current is higher than DC at high V_{DS} (Fig. 3 (a)) for both gate and drain lag measurements. The increased current can be attributed to reduced self heating effect. Absence of current collapse means that there is possibly no traps under gate or in gate-drain access region^{15,17}. Pulsed I_D - V_{GS} transfer curves shows no shift in threshold voltage for high $V_{DG,Q}$ quiescent bias points (Fig. 3 (b)). This suggests that there are possibly no traps under gate or in the access region in the as deposited Al_2O_3 . However, after repeated DC, RF and large signal measurements, we observed current collapse under pulsed measurements (See Supplementary Material). Electrical stressing may have introduced traps either in the oxide/channel or oxide/air interface. An extrinsic passivation may be necessary to reduce this DC-RF dispersion caused by electrical stressing the device.

Small-signal analysis was performed from 100 MHz to 19 GHz using Keysight ENA 5071C Vector Network Analyzer (VNA). A sapphire calibration standard was used to calibrate The VNA by SOLT technique. An isolated open-pad device structure on the same wafer was utilized to de-embed parasitic pad capacitance²³. Short circuit current gain (h_{21}), Mason's unilateral gain (U) and MAG/MSG have been plotted at $V_{DS} = 12$ V and $V_{GS} = 2$ V bias points for $L_G = 90$ nm device. After extrapolating to 0 dB, we found current gain cut-off frequency (f_i) of ~ 27 GHz. The power gain cut off frequency (f_{MAX}) is ~ 55 GHz (Fig. 4) which extrapolated from 20dB/decade slope from the Mason's unilateral gain (U). f_{MAX} value reported here is the highest among Ga_2O_3 FETs. We calculated the expected intrinsic f_T using the geometrically calculated gate source capacitance C_{GS} and measured DC g_m (See supplementary materials). We assumed half of the channel thickness (30 nm) for C_{GS} calculation. We also calculated extrinsic f_T by considering R_S , R_D calculated from channel sheet resistance and contact resistance. These calculations²⁴ gave an intrinsic and extrinsic f_T of 29 GHz and 25.5 GHz respectively. This calculation gives further credence to the measured f_T and f_{MAX} . In our previous report¹⁰, we found DC-RF dispersion and reduced high frequency g_m was the primary cause of reduced f_T .

We calculated f_{MAX} based on T gate dimension²⁴. Although we do not have any test structure to calculate exact gate resistance (R_G), nonetheless our calculation results in f_{MAX} 90 GHz which is higher than our measured data. The discrepancy can be attributed to the higher gate resistance arising from thin metal films and errors in unilateral gain (U) extraction from measured s-parameters. f_{MAX}/f_T ratio of 1.8 has

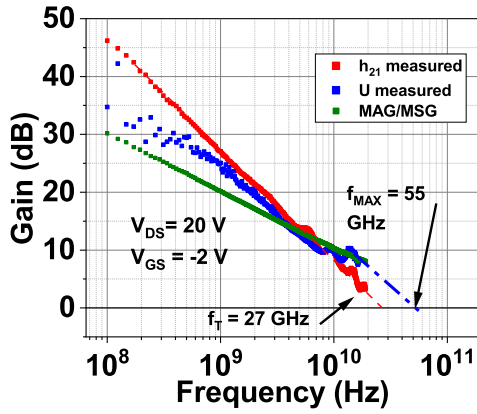


FIG. 4. Measured small signal performance of a test device ($L_G = 90$ nm) showing $f_T = 27$ GHz and $f_{MAX} = 55$ GHz

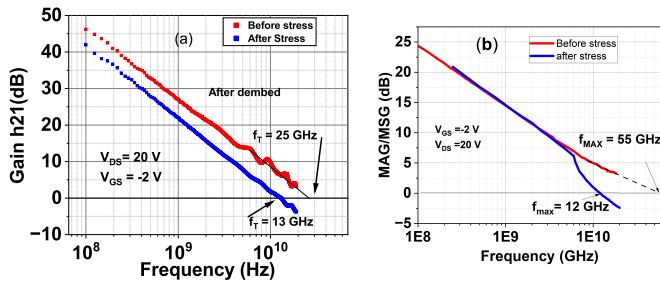


FIG. 5. Degradation of (a) f_T and (b) f_{MAX} after DC, large signal RF measurement (stress)

been extracted which is similar to our previous report¹⁰ and other reports (3 to 5)^{11,25,26} in the literature.

Large signal measurements were attempted on the MOSFETs, however good input matching could not be achieved, thus no large signal data is available. Moreover, we found degradation of both f_T and f_{MAX} after repeated DC and large-signal RF measurements. f_T dropped to 13 GHz from 25 GHz and f_{MAX} dropped to 12 GHz after DC and large signal measurements (Fig. 5(a) and (b)). Similar characteristics was also observed for all devices; repeated measurements degraded device RF performance significantly (See Supplementary materials). After electrical stressing, the RF g_m was lower than DC g_m resulting in the f_T and f_{MAX} degradation. Pulsed I-V measurements showed current collapse after stressing. Possible trap introduction after repeated DC and large signal measurement may be the primary reason for this. It is noted that these devices did not have the typical external passivation that is used in RF GaN HEMTs. Successful external passivation could mitigate this degradation by electrical stressing. A more careful analysis is necessary to really understand the origin of the degradation of the device.

Nevertheless, we calculated Johnson's Figure of Merit (JFOM) based on the breakdown voltage and f_T (un-stressed values). With 125 V breakdown voltage (V_{BR}) and 27 GHz f_T , a $f_T \cdot V_{BR}$ product of 3.375 GHz.V is achieved, which is comparable to the state-of-art GaN HEMTs (Fig.6(a)). We also bench-marked f_{MAX} and breakdown voltage (V_{BR}) of our

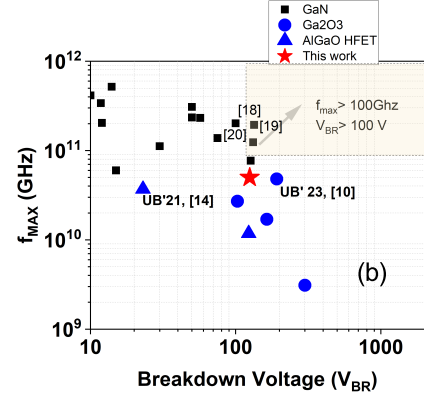
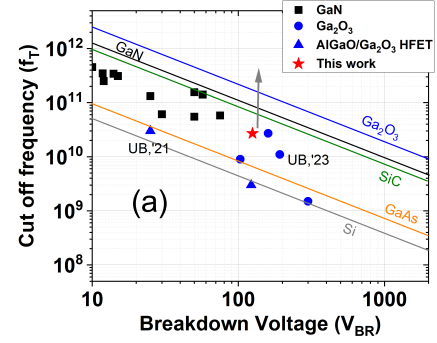


FIG. 6. (a) f_T vs V_{BR} benchmark plot with GaN and other β -Ga₂O₃ devices, (b) f_{MAX} vs V_{BR} benchmark plot with GaN and other β -Ga₂O₃ devices,

device with GaN HEMTs. As seen in Fig. 6(b), this is the only β -Ga₂O₃ device that shows $f_{MAX} 55$ GHz and $V_{BR} > 100$ V (Fig. 6(b)) except for a few AlGaO/GaN HEMTs.

In summary, we have demonstrated a 90 nm T gate β -Ga₂O₃ MOSFET with process optimization to eliminate the regrowth interface resistance. We extracted near 55 GHz f_{MAX} , highest among β -Ga₂O₃ devices, with a gate-to-drain breakdown voltage of 125 V. However, degradation of f_T and f_{MAX} and current collapse were observed in these un-passivated devices after large signal measurement trials which are possibly caused by trap introduction after repeated DC and RF measurements. Nevertheless, the high f_{MAX} is a significant achievement in terms of prospective applications of β -Ga₂O₃ in X band.

SUPPLEMENTARY MATERIAL

See the supplementary material for breakdown analysis, a detailed discussion on RF performance degradation before and after repeated DC, RF measurement. Scatter plot showing degradation of f_T , f_{MAX} after different measurements for 5 different devices, pulsed IV measurement for 200 ns pulse width for different bias points showing current collapse after stressing the device.

ACKNOWLEDGMENTS

We acknowledge the support from AFOSR (Air Force Office of Scientific Research) under award FA9550-18-1-0479 (Program Manager: Ali Sayir), from NSF under awards ECCS 2019749, 2231026 from Semiconductor Research Corporation under GRC Task ID 3007.001, and II-VI Foundation Block Gift Program. This work used the electron beam lithography system acquired through NSF MRI award ECCS 1919798. We would like to thank Dr. Andrew Green and Dr. Neil Moser from the Air Force Research Laboratories for their help in large signal measurements.

DATA AVAILABILITY STATEMENT

The data that support the findings of this study are available from the corresponding author upon reasonable request.

I. REFERENCES

- ¹A. J. Green, J. Speck, G. Xing, P. Moens, F. Allerstam, K. Gumaelius, T. Neyer, A. Arias-Purdue, V. Mehrotra, A. Kuramata, *et al.*, “ β -gallium oxide power electronics,” *APL Materials* **10**, 029201 (2022).
- ²A. J. Green, K. D. Chabak, E. R. Heller, R. C. Fitch, M. Baldini, A. Fiedler, K. Irmscher, G. Wagner, Z. Galazka, S. E. Tetlak, A. Crespo, K. Leedy, and G. H. Jessen, “3.8-MV/cm breakdown strength of MOVPE-grown Sn-doped β -Ga₂O₃ MOSFETs,” *IEEE Electron Device Letters* **37**, 902–905 (2016).
- ³K. Ghosh and U. Singiseti, “Ab initio velocity-field curves in monoclinic β -Ga₂O₃,” *Journal of Applied Physics* **122**, 035702 (2017).
- ⁴K. Zeng, A. Vaidya, and U. Singiseti, “1.85 kV breakdown voltage in lateral field-plated β -Ga₂O₃,” *IEEE Electron Device Letters* **39**, 1385–1388 (2018).
- ⁵K. Tetzner, E. B. Treidel, O. Hilt, A. Popp, S. B. Anooz, G. Wagner, A. Thies, K. Ickert, H. Gargouri, and J. Würfl, “Lateral 1.8 kV β -Ga₂O₃ mosfet with 155 mw/cm² power figure of merit,” *IEEE Electron Device Letters* **40**, 1503–1506 (2019).
- ⁶A. Bhattacharyya, S. Roy, P. Ranga, C. Peterson, and S. Krishnamoorthy, “High-mobility tri-gate β -Ga₂O₃ MESFETs with a power figure of merit over 0.9 GW/cm²,” *IEEE Electron Device Letters* **43**, 1637–1640 (2022).
- ⁷J. Zhang, P. Dong, K. Dang, Y. Zhang, Q. Yan, H. Xiang, J. Su, Z. Liu, M. Si, J. Gao, *et al.*, “Ultra-wide bandgap semiconductor ga₂o₃ power diodes,” *Nature communications* **13**, 3900 (2022).
- ⁸E. Farzana, F. Alema, W. Y. Ho, A. Mauze, T. Itoh, A. Osinsky, and J. S. Speck, “Vertical β -Ga₂O₃ field plate schottky barrier diode from metal-organic chemical vapor deposition,” *Applied Physics Letters* **118**, 162109 (2021).
- ⁹N. K. Kalarickal, Z. Xia, H.-L. Huang, W. Moore, Y. Liu, M. Brenner, J. Hwang, and S. Rajan, “ β -(Al_{0.18}Ga_{0.82})₂O₃ double heterojunction transistor with average field of 5.5 MV/cm,” *IEEE Electron Device Letters* **42**, 899–902 (2021).
- ¹⁰C. N. Saha, A. Vaidya, A. F. M. A. U. Bhuiyan, L. Meng, S. Sharma, H. Zhao, and U. Singiseti, “Scaled β -Ga₂O₃ thin channel MOSFET with 5.4 MV/cm average breakdown field and near 50 GHz f_{MAX} ,” *Applied Physics Letters* **122**, 182106 (2023).
- ¹¹Y. Zhang, A. Neal, Z. Xia, C. Joishi, J. M. Johnson, Y. Zheng, S. Bajaj, M. Brenner, D. Dorsey, K. Chabak, G. Jessen, J. Hwang, S. Mou, J. P. Heremans, and S. Rajan, “Demonstration of high mobility and quantum transport in modulation-doped β -(Al_xGa_{1-x})₂O₃ heterostructures,” *Applied Physics Letters* **112**, 173502 (2018).
- ¹²K. Chabak, D. Walker, A. Green, A. Crespo, M. Lindquist, K. Leedy, S. Tetlak, R. Gilbert, N. Moser, and G. Jessen, “Sub-micron gallium oxide radio frequency field-effect transistors,” in *2018 IEEE MTT-S International Microwave Workshop Series on Advanced Materials and Processes for RF and THz Applications (IMWS-AMP)* (IEEE, 2018) pp. 1–3.
- ¹³Z. Xia, H. Xue, C. Joishi, J. Mcglone, N. K. Kalarickal, S. H. Sohail, M. Brenner, A. Arehart, S. Ringel, S. Lodha, W. Lu, and S. Rajan, “ β -Ga₂O₃ delta-doped field-effect transistors with current gain cutoff frequency of 27 GHz,” *IEEE Electron Device Letters* **40**, 1052–1055 (2019).
- ¹⁴A. Vaidya, C. N. Saha, and U. Singiseti, “Enhancement mode β -(Al_xGa_{1-x})₂O₃/Ga₂O₃ heterostructure FET (HFET) with high transconductance and cutoff frequency,” *IEEE Electron Device Letters* **42**, 1444–1447 (2021).
- ¹⁵C. N. Saha, A. Vaidya, and U. Singiseti, “Temperature dependent pulsed IV and RF characterization of β -(Al_xGa_{1-x})₂O₃/Ga₂O₃ hetero-structure FET with ex situ passivation,” *Applied Physics Letters* **120**, 172102 (2022).
- ¹⁶N. A. Moser, T. Asel, K. J. Liddy, M. Lindquist, N. C. Miller, S. Mou, A. Neal, D. E. Walker, S. Tetlak, K. D. Leedy, *et al.*, “Pulsed power performance of β -Ga₂O₃ mosfets at l-band,” *IEEE Electron Device Letters* **41**, 989–992 (2020).
- ¹⁷A. Vaidya and U. Singiseti, “Temperature-dependent current dispersion study in β -Ga₂O₃ fets using submicrosecond pulsed I-V characteristics,” *IEEE Transactions on Electron Devices* **68**, 3755–3761 (2021).
- ¹⁸Y. Zhang, K. Wei, S. Huang, X. Wang, Y. Zheng, G. Liu, X. Chen, Y. Li, and X. Liu, “High-temperature-recessed millimeter-wave algan/gan hems with 42.8% power-added-efficiency at 35 ghz,” *IEEE Electron Device Letters* **39**, 727–730 (2018).
- ¹⁹K. Ranjan, S. Arulkumaran, G. I. Ng, and S. Vicknesh, “High johnson’s figure of merit (8.32 thz·v) in 0.15- μ m conventional t-gate algan/gan hems on silicon,” *Applied Physics Express* **7**, 044102 (2014).
- ²⁰F. Medjdoub, B. Grimbert, D. Ducatteau, and N. Rolland, “Record combination of power-gain cut-off frequency and three-terminal breakdown voltage for gan-on-silicon devices,” *Applied Physics Express* **6**, 044001 (2013).
- ²¹A. Vaidya, J. Sarker, Y. Zhang, L. Lubecki, J. Wallace, J. D. Poplawsky, K. Sasaki, A. Kuramata, A. Goyal, J. A. Gardella, and U. Singiseti, “Structural, band and electrical characterization of β -(Al_{0.19}Ga_{0.81})₂O₃ films grown by molecular beam epitaxy on sn doped β -Ga₂O₃ substrate,” *Journal of Applied Physics* **126**, 095702 (2019).
- ²²A. Bhattacharyya, P. Ranga, S. Roy, C. Peterson, F. Alema, G. Seryogin, A. Osinsky, and S. Krishnamoorthy, “Multi-kv class β -Ga₂O₃ MESFETs with a lateral figure of merit up to 355 MW/cm²,” *IEEE Electron Device Letters* **42**, 1272–1275 (2021).
- ²³M. Koolen, J. Geelen, and M. Versleijen, “An improved de-embedding technique for on-wafer high-frequency characterization,” in *Proceedings of the 1991 Bipolar Circuits and Technology Meeting* (1991).
- ²⁴P. J. Tasker and B. Hughes, *IEEE Electron Device Letters* **10**, 291–293 (1989).
- ²⁵T. Kamimura, Y. Nakata, and M. Higashiwaki, “Delay-time analysis in radio-frequency β -Ga₂O₃ field effect transistors,” *Applied Physics Letters* **117**, 253501 (2020).
- ²⁶A. J. Green, K. D. Chabak, M. Baldini, N. Moser, R. Gilbert, R. C. Fitch, G. Wagner, Z. Galazka, J. Mccandless, A. Crespo, K. Leedy, and G. H. Jessen, “ β -Ga₂O₃ mosfets for radio frequency operation,” *IEEE Electron Device Letters* **38**, 790–793 (2017).
- ²⁷A. Kuramata, K. Koshi, S. Watanabe, Y. Yamaoka, T. Masui, and S. Yamakoshi, “High-quality β -Ga₂O₃ single crystals grown by edge-defined film-fed growth,” *Japanese Journal of Applied Physics* **55**, 1202A2 (2016).
- ²⁸Z. Galazka, R. Uecker, D. Klimm, K. Irmscher, M. Naumann, M. Pietsch, A. Kwasniewski, R. Bertram, S. Ganschow, and M. Bickermann, “Scaling-up of bulk β -Ga₂O₃ single crystals by the czochralski method,” *ECS Journal of Solid State Science and Technology* **6**, Q3007 (2016).
- ²⁹W. Tang, Y. Ma, X. Zhang, X. Zhou, L. Zhang, X. Zhang, T. Chen, X. Wei, W. Lin, D. H. Mudiyansele, H. Fu, and B. Zhang, “High-quality (001) β -Ga₂O₃ homoepitaxial growth by metalorganic chemical vapor deposition enabled by in situ indium surfactant,” *Applied Physics Letters* **120**, 212103 (2022).
- ³⁰K. Sasaki, A. Kuramata, T. Masui, E. G. Villora, K. Shimamura, and S. Yamakoshi, “Device-quality β -Ga₂O₃ epitaxial films fabricated by ozone molecular beam epitaxy,” *Applied Physics Express* **5**, 035502 (2012).
- ³¹J. Leach, K. Udway, J. Rumsey, G. Dodson, H. Splawn, and K. Evans, “Halide vapor phase epitaxial growth of β -ga₂o₃ and α -ga₂o₃ films,” *APL Materials* **7**, 022504 (2019).

- ³²H. Zhou, S. Alghmadi, M. Si, G. Qiu, and P. D. Ye, "Al₂O₃/β-Ga₂O₃(-201) interface improvement through piranha pretreatment and postdeposition annealing," *IEEE Electron Device Letters* **37**, 1411–1414 (2016).
- ³³C. Wang, H. Zhou, J. Zhang, W. Mu, J. Wei, Z. Jia, X. Zheng, X. Luo, X. Tao, and Y. Hao, "Hysteresis-free and μ s-switching of D/E-modes β-Ga₂O₃ hetero-junction FETs with the BV²/Ron, sp of 0.74/0.28 GW/cm²," *Applied Physics Letters* **120**, 112101 (2022).
- ³⁴A. E. Islam, C. Zhang, K. DeLello, D. A. Muller, K. D. Leedy, S. Ganguli, N. A. Moser, R. Kahler, J. C. Williams, D. M. Dryden, *et al.*, "Defect engineering at the Al₂O₃ (010)/β-Ga₂O₃ interface via surface treatments and forming gas post-deposition anneals," *IEEE Transactions on Electron Devices* **69**, 5656–5663 (2022).
- ³⁵G. Meneghesso, M. Meneghini, D. Bisi, I. Rossetto, A. Cester, U. K. Mishra, and E. Zanoni, "Trapping phenomena in AlGaIn/GaNHEMTs: A study based on pulsed and transient measurements," *Semiconductor science and technology* **28**, 074021 (2013).